


## Removal of Intrawall Pores in SBA-15 by Selective Modification

Nina Reichhardt,<sup>†,§,\*</sup> Tomas Kjellman,<sup>†</sup> Motolani Sakeye,<sup>‡</sup> Filip Paulsen,<sup>†</sup> Jan-Henrik Smått,<sup>‡</sup> Mika Lindén,<sup>‡</sup> and Viveka Alfredsson<sup>†</sup>

<sup>†</sup>Physical Chemistry, Lund University, P.O. Box 124, SE-221 00 Lund, Sweden

<sup>§</sup>MEMPHYS - Center for Biomembrane Physics, Department of Physics and Chemistry, University of Southern Denmark, Campusvej 55, DK-5230 Odense M, Denmark

<sup>‡</sup>Center for Functional Materials, Laboratory of Physical Chemistry, Department of Natural Sciences, Åbo Akademi University, Porthansgatan 3-5, FIN-20500 Turku, Finland

 Supporting Information

**KEYWORDS:** SBA-15, intrawall porosity, N<sub>2</sub>-sorption, mesoporous, Pluronic, silica

Ordered mesostructured materials became a dynamic research field in the beginning of the 1990s with the advent of the mesostructured silica MCM-41<sup>1</sup> and the similar material FSM-16.<sup>2</sup> These materials are characterized by a 2D hexagonal structure (plane group *p6m*) with order on the mesoscopic length scale and well-defined pore geometry. The synthesis of the silica material SBA-15 marks another important development in this research field.<sup>3</sup> SBA-15, defined by the same plane group as MCM-41 and FSM-16, is however a very different material compared to both of the seminal materials. While the wall thickness of MCM-41 and FSM-16 is on the order of 1 nm and therefore not very stable, the walls of SBA-15 have a considerable thickness (around 4 to 6 nm), which provides higher stability of the material. It is hence often more interesting to use SBA-15 in various applications. Another significant difference between the seminal mesostructured materials and SBA-15 lies in the geometry of the pore system. MCM-41 and FSM-16 have a single pore system, with cylindrical channels with a spherical to hexagonal cross section. These channels are not interconnected. SBA-15 on the other hand has a complicated biporous system with large mesopores, here referred to as primary mesopores, connected via additional pores in the silica walls.<sup>4</sup> The presence of these intrawall pores is a result of the formation process (see below).

Ordered mesostructured silica materials form in a cooperative self-assembly process with amphiphilic molecules interacting with siliceous species. The attractive interaction leads to a phase separation of a concentrated phase, consisting of amphiphile micellar aggregates in a silica and water matrix, and a dilute aqueous phase. For SBA-15 and other materials formed in the presence of Pluronic triblock copolymers, the formation relies on the attractive interaction between the poly(ethylene oxide) (PEO) part of the polymer and the siliceous oligomers/polymers in the solution. The PEO part of the polymer becomes embedded in the silica matrix,<sup>5</sup> and upon removal of the polymer (simply done by calcination), smaller pores inside the silica wall (intrawall pores) are created as a cast of the PEO part. The primary mesopores are created mainly from the micellar core, hence, predominately from the poly(propylene oxide) part of the Pluronic molecules. The intrawall pores connect to some extent the primary mesopores,<sup>4</sup> and in this sense SBA-15 is a

bicontinuous material. The pore size of the intrawall pores ranges from micro- to mesopores, and their presence gives SBA-15 different properties from the single pore system 2D hexagonal silicas. The biporous nature can be an advantage. However, in some applications it may be preferable not to have additional intrawall porosity. For example, small intrawall pores may contain catalytically active species nonaccessible for bulkier substrates. For chromatographic applications, intrawall pores may lead to unwanted signal tailing effects. In addition, it is often observed that the intrawall pores are the first to be filled when aiming at surface functionalization of the mesopore walls by in situ polymerization, which may be beneficial<sup>6</sup> or not<sup>7</sup> depending on the application.

There have been a number of reports discussing the intrawall porosity of SBA-15 and related materials;<sup>8</sup> for instance, Galarneau et al.<sup>8a</sup> reported on the removal of micropores where instead the number of secondary (intrawall) mesopores increased and the size of primary mesopores was also influenced. But, to the best of our knowledge, to selectively remove the intrawall porosity while retaining the other properties of SBA-15 has not previously been reported.

Here we demonstrate a straightforward way to remove the intrawall porosity, while maintaining the other characteristics of SBA-15 (primary mesopore size, wall thickness, particle size, and morphology). Removal is simply done by adding NaI to the ongoing synthesis. The strategy is to selectively influence the interaction between the developing silica framework and the PEO part of the Pluronic polymer. I<sup>-</sup> is known to associate with PEO, typically increasing its solubility in water.<sup>9</sup> It is thus expected that the presence of the anions will have an effect on the interaction between the PEO and the siliceous species, therefore influencing the penetration depth of PEO chains in the silica walls. SBA-15 was synthesized at 55 °C according to the method previously reported (see Supporting Information).<sup>10</sup> We used Pluronic P104 as this polymer gives rise to a well-defined material that also serves as an excellent model system. The particle size and morphology, in addition to the structure, are well-defined,

**Received:** February 18, 2011

**Revised:** June 30, 2011

**Published:** July 11, 2011

and hence changes in the system can easily be monitored. Further, to the best of our knowledge P104 ((EO)<sub>27</sub>(PO)<sub>61</sub>(EO)<sub>27</sub>) does not give rise to the bicontinuous cubic silica structure that P123 ((EO)<sub>20</sub>(PO)<sub>70</sub>(EO)<sub>20</sub>) and P103 ((EO)<sub>17</sub>(PO)<sub>59</sub>(EO)<sub>17</sub>) can generate in the presence of NaI.<sup>11</sup> In addition, P104 has longer EO-units than P103 and P123, thus giving rise to a larger fraction of intrawall porosity and consequently the easier monitoring of changes in this property.

The synthesis of SBA-15 was initiated by addition of tetramethyl orthosilicate, and at 30 min, 4 h, and 24 h, respectively, into the synthesis NaI was added (final concentration: 1.0 M). The syntheses were left on the bench for a total of 24 h after which they were hydrothermally treated (at 80 °C for 24 h). The synthesis to which NaI was added at 24 h was hence hydrothermally treated immediately following the addition. The material was subsequently calcined (at 500 °C for 6 h) according to the conventional procedure.<sup>10</sup> A reference material without NaI was also prepared. The samples are referred to as SBA-15\_X where X indicates the time in hours of the addition of NaI while the reference sample is denoted SBA-15\_ref.

The calcined materials were investigated regarding porosity with nitrogen sorption; the structure was analyzed with small-angle X-ray diffraction, and the particle size and morphology were analyzed with SEM.<sup>19</sup> Carbon replicas of SBA-15\_ref and SBA-15\_4 were prepared<sup>12</sup> and investigated with TEM (see Supporting Information).

The formation of SBA-15 is probably the most studied process of formation of mesostructured materials. A wide range of techniques, several of which have been performed in situ, have been employed to follow the dynamics of the process.<sup>5,10,13</sup> From the work of Linton et al.<sup>10,14</sup> we have obtained a timeline of events<sup>10</sup> for the formation of SBA-15 with Pluronic P104 serving as the structure directing amphiphile. With this knowledge at hand it is possible to target a specific step in the formation and influence this particular step more or less uniquely. This was previously shown when the morphology/particle size of SBA-15 was changed by additions at a particular time of the formation.<sup>15</sup> The timing was in that case critical due to the unusual growth behavior of platelike SBA-15 particles.<sup>14</sup> Here the aim is to influence the interaction of PEO and the silica species, a process open to manipulation for a longer period and with less time restriction. Nevertheless, timing is important, as we only want to manipulate the intrawall porosity and not other material characteristics dependent on this interaction. We allow the material to form as SBA-15, with its distinct symmetry, incipient porosity, particle size, and morphology, and thereafter the interaction is manipulated so as to influence only the targeted property (i.e., at a later stage than when the particle size is controlled). The interaction between siliceous species and PEO is present during the whole synthesis but will, as time progresses, be less prone to change due to increased connectivity of the silica network.<sup>5</sup> It is also expected that early on in the synthesis, when the silica connectivity is low, the whole system can respond, as explained above. The aim is to influence the synthesis when the structure has formed and to some extent settled, but while the system is still responsive, i.e., behaves as a “soft matter system”. The material has essentially formed (structure established and particles formed) within the first 20 min,<sup>10</sup> and normally the synthesis is left on the bench for 24 h before hydrothermal treatment and subsequent calcination.

The well-defined structure of SBA-15 (Figure 1) was obtained in all syntheses to which NaI was added. The SAXD patterns

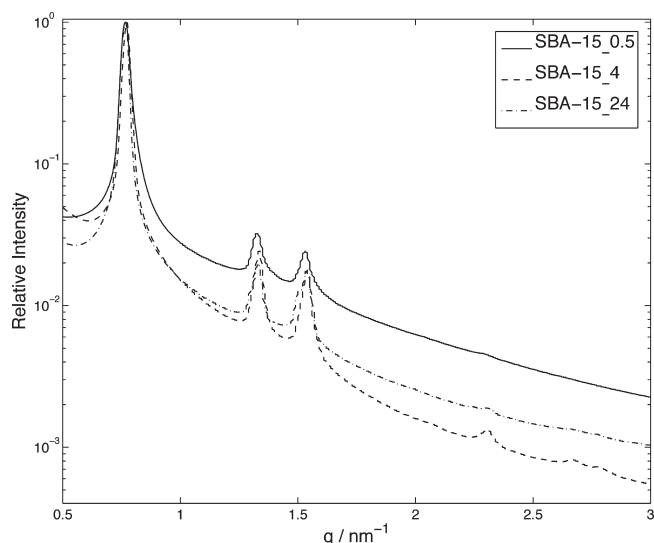


**Figure 1.** SAXD patterns of the SBA-15 materials synthesized with addition of NaI at three different times.

**Table 1.** Structural Properties of SBA-15 Silica Samples<sup>a</sup>

name	BET,			$V_i/V_t$ , %	$D_{Des}$ , nm	$a_0$ , nm
	$m^2/g$	$V_t$ , $cm^3/g$	$V_i$ , $cm^3/g$			
SBA-15_0.5	898	1.02	0.25	24.5	6.6	9.5
SBA-15_4	408	0.63	0.05	7.9	6.8	9.4
SBA-15_24	670	0.75	0.20	26.7	6.3	9.5
SBA-15_ref	1000	0.97	0.35	36.1	6.6	10.0

<sup>a</sup>  $V_t$  is the total pore volume,  $V_i$  the intrawall pore volume,  $D_{Des}$  the primary mesopore diameter and  $a_0$  the unit cell parameter.

show three to six peaks, which can be indexed on the 2D hexagonal lattice (plane group  $p6m$ ). SBA-15\_4 gives the most well-defined SAXD pattern with six distinct peaks. The unit cell parameters observed for the NaI samples are slightly smaller compared to SBA-15\_ref. A possible explanation is an increase of silica wall density as a response to the decrease in intrawall pore volume.

The results from the nitrogen sorption are shown in Table 1 and Figures 2 and 3. The isotherms (Figure 2) display the characteristic type-IV behavior exhibiting a marked hysteresis and typical expected high surface area and pore volume (Table 1). The fraction of pores, as a function of pore diameter, is shown in the cumulative pore volume distribution (PVD) plot (Figure 3) where the primary mesopores are identified by the step in the function around diameters of 5.9–6.8 nm. All pores smaller than the primary mesopores (<5.9 nm) are considered as intrawall pores. Table 1 shows the percentage of intrawall pores to the total pore volume. The surface area for materials with NaI-additions (Table 1) decreased compared to SBA-15\_ref. The cumulative PVD (Figure 3) shows that this decrease is mainly caused by the loss of the intrawall pore volume. Hence, regardless of time (at least between 0.5 and 24 h) NaI prompts for intrawall porosity decrease. Even so, there is a marked difference of efficiency of the additions depending on time. Addition made 4 h after TMOS addition (SBA-15\_4) is clearly the most effective. The intrawall porosity has decreased to almost 8% from the original 36% (Table 1) and, as shown in Figure 3, the removal of pores up to diameters of around 5 nm is almost complete. The  $t$ -plots confirm

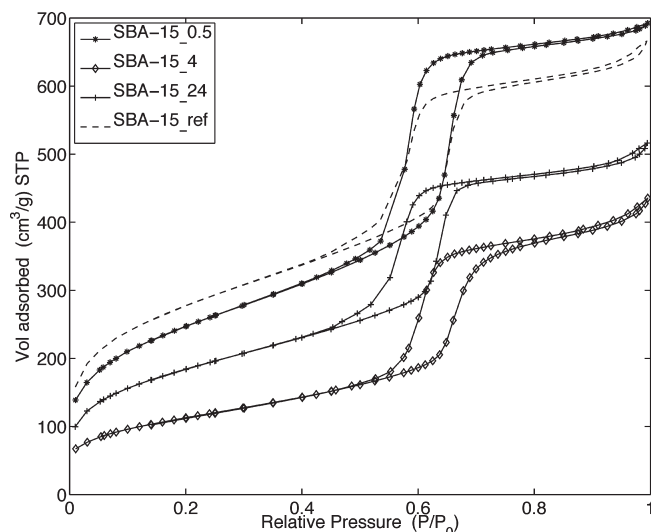


**Figure 2.**  $N_2$ -isotherms of the SBA-15 materials synthesized with addition of NaI at three different times and the reference material.

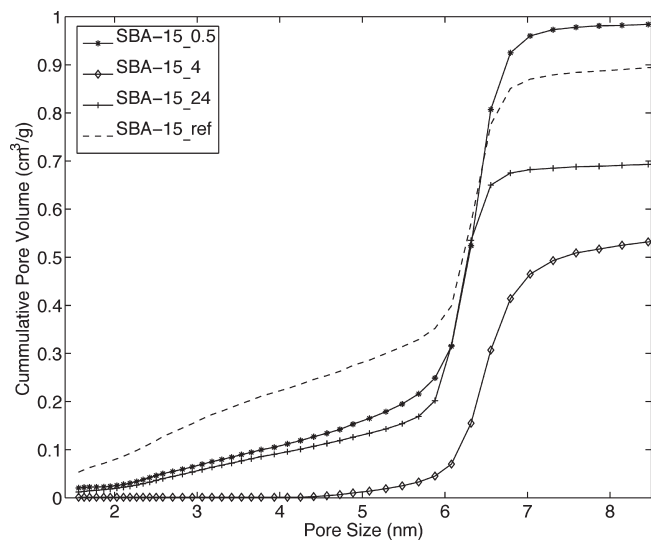


**Figure 3.** Cumulative pore volume distribution of the SBA-15 materials synthesized with addition of NaI at three different times and the reference material. SBA-15\_4 shows no pores up to 5 nm.

these observations (see Supporting Information). A slightly larger pore size distribution of the mesopores can be discerned (Figures 2 and 3) for SBA-15\_4. We infer this to be a consequence of the space occupied by the Pluronic micelles, which are expected to change as the PEO part is pulled out of the wall. As the silica polymerizes the mesopore walls may get slightly uneven. However, the diffraction data clearly shows that the structure as a whole is not affected. The clear diffraction pattern indicates better order/contrast in the SBA-15\_4 compared to the other materials. This is consistent with higher electron density in the walls (i.e., lack of intrawall porosity).

Comparison of SEM micrographs of SBA-15\_4 and SBA-15\_ref (see Supporting Information) clearly demonstrates that other material properties are unaffected by the additions. The additions have thus selectively targeted only intrawall characteristics and not other properties dependent on the interaction

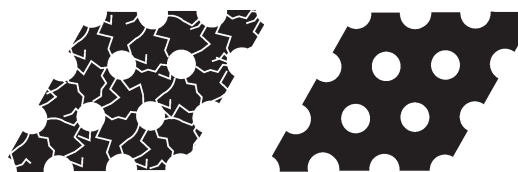


**Figure 4.** Schematic representation of SBA-15 formed under conventional conditions (left) and with NaI addition at the appropriate time (right); note intrawall pores for simplicity depicted with uniform pore size.

between the PEO and the siliceous species. The carbon replica (see Supporting Information) of SBA-15\_ref viewed along and perpendicular to the direction of the hexagonal pattern shows the typical well ordered structure. For SBA-15\_4 the carbon replica shows a shell-like structure, which suggests that the intrawall pores, required to maintain the ordered framework, are missing. The shell structure is stabilized by a carbon layer formed on the outer surface of the silica.<sup>16</sup>

Here we report on a simple way for elimination of the intrawall pores (up to 5 nm) in SBA-15 without changing other properties of the material. This gives a material with unconnected primary mesopores (see Figure 4). Hence, it is a material analogue to MCM-41 but with larger pores and thicker silica walls.

The intrawall pores are eliminated by adding NaI to the ongoing SBA-15 synthesis. Additions need to be performed at a time where the structure of SBA-15 is stable but the silica connectivity not fully developed. Addition at 30 min into the synthesis was too early. Addition at 4 h gave much lower intrawall porosity than addition made at 24 h. There is hence an optimal timing even if not critical. It is expected that by this process it should be possible to remove the intrawall porosity in all mesostructured silica materials formed with PEO-based amphiphiles. If so, then there will be ample opportunities to combine this methodology with previously reported methods, for example, pore size increasing operations,<sup>18</sup> to achieve materials with controllable porosity.

## ■ ASSOCIATED CONTENT

**S Supporting Information.** SEM micrographs of SBA-15\_4 and SBA-15\_ref, SAXD of SBA-15\_ref, TEM micrographs of the carbon replica, *t*-plots, and a detailed synthesis description (PDF). This material is available free of charge via the Internet at <http://pubs.acs.org>.

## ■ AUTHOR INFORMATION

### Corresponding Author

\*E-mail: [nina.reichhardt@fkem1.lu.se](mailto:nina.reichhardt@fkem1.lu.se)

## ■ ACKNOWLEDGMENT

Financial support by the Swedish Research Council (VR) through the Linnaeus grant Organizing Molecular Matter center of excellence (239-2009-6794, NR, VA, TK), through project grants (80475801, VA), Marie-Curie Research Training Network BIOCONTROL (MRTN-CT-2006 033439, VA, NR), and the Swedish Foundation for Strategic Research (RMA08-0056, VA, TK) is acknowledged. The Academy of Finland (127919, MS, JHS) is also gratefully acknowledged. We thank Prof. Ryo (KAIST) and Prof. Lidin (Lund University) for advice on the carbon replica procedure.

## REFERENCES

- (1) Kresge, C. T.; Leonowicz, M. E.; Roth, W. J.; Vartuli, J. C.; Beck, J. S. *Nature* **1992**, 359, 710.
- (2) Inagaki, S.; Fukushima, Y.; Kuroda, K. *J. Chem. Soc., Chem. Commun.* **1993**, 8, 680.
- (3) Zhao, D.; Huo, Q.; Feng, J.; Chmelka, B. F.; Stucky, G. D. *J. Am. Chem. Soc.* **1998**, 120, 6024.
- (4) (a) Ryoo, R.; Ko, C. H.; Kruk, M.; Antochshuk, V.; Jaroniec, M., *J. Phys. Chem. B* **2000**, 104, 11465. (b) Fan, J.; Yu, C.; Wang, L.; Tu, B.; Zhao, D.; Sakamoto, Y.; Terasaki, O. *J. Am. Chem. Soc.* **2000**, 123, 12113.
- (5) Ruthstein, S.; Frydman, V.; Kababya, S.; Landau, M.; Goldfarb, D. *J. Phys. Chem. B* **2003**, 107, 1739.
- (6) Choi, M.; Kleitz, F.; Liu, D.; Lee, H. Y.; Ahn, W.; Ryoo, R. *J. Am. Chem. Soc.* **2005**, 127, 1924.
- (7) Rosenholm, J. M.; Lindén, M. *Chem. Mater.* **2007**, 19, 5023.
- (8) (a) Galarneau, A.; Cambon, H.; Di Renzo, F.; Fajula, F. *Langmuir* **2001**, 17, 8328. (b) Newalkar, B. L.; Komarneni, S. *Chem. Mater.* **2001**, 13, 4573. (c) Miyazawa, K.; Inagaki, S. *Chem. Commun.* **2000**, 21, 2121. (d) Mascotto, S.; Wallacher, D.; Brandt, A.; Haus, T.; Thommes, M.; Zickler, G. A.; Funari, S. S.; Timmann, A.; Smarsly, B. M. *Langmuir* **2009**, 25, 12670. (e) Yang, C.-M.; Zibrowius, B.; Schmidt, W.; Schueth, F. *Chem. Mater.* **2003**, 15, 3739. (f) Choi, M.; Heo, W.; Kleitz, F.; Ryoo, R. *Chem. Commun.* **2003**, 12, 1340.
- (9) Kabalnov, A.; Olsson, U.; Wennerström, H. *J. Phys. Chem.* **1995**, 99, 6220.
- (10) Linton, P.; Rennie, A. R.; Zackrisson, M.; Alfredsson, V. *Langmuir* **2009**, 25, 4685.
- (11) Flodström, K.; Alfredsson, V.; Källrot, N. *J. Am. Chem. Soc.* **2003**, 125, 4402.
- (12) Joo, S. H.; Choi, S. J.; Oh, I.; Kwak, J.; Liu, Z.; Terasaki, O.; Ryoo, R. *Nature* **2001**, 412, 169.
- (13) (a) Flodström, K.; Teixeira, C. V.; Amenitsch, H.; Alfredsson, V.; Lindén, M. *Langmuir* **2004**, 20, 4885. (b) Zholobenko, V. L.; Khodakov, A. Y.; Impéror-Clerc, M.; Durand, D.; Grillo, I. *Adv. Colloid Interface Sci.* **2008**, 142, 67.
- (14) Linton, P.; Alfredsson, V. *Chem. Mater.* **2008**, 20, 2878.
- (15) Linton, P.; Wennerstrom, H.; Alfredsson, V. *Phys. Chem. Chem. Phys.* **2010**, 12, 3852.
- (16) Tian, B.; Che, S.; Liu, Z.; Liu, X.; Fan, W.; Tatsumi, T.; Terasaki, O.; Zhao, D. *Chem. Commun.* **2003**, 21, 2726.
- (17) (a) Cerenius, Y.; Ståhl, K.; Svensson, L. A.; Ursby, T.; Oskarsson, Å.; Albertsson, J.; Liljas, A. *J. Synchrotron Radiat.* **2000**, 7, 203. (b) Knaapila, M.; Svensson, C.; Barauskas, J.; Zackrisson, M.; Nielsen, S. S.; Toft, K. N.; Vestergaard, B.; Arleth, L.; Olsson, U.; Pedersen, J. S.; Cerenius, Y. *J. Synchrotron Radiat.* **2009**, 16, 498.
- (18) (a) Boissière, C.; Larbot, A.; van der Lee, A.; Kooyman, P. J.; Prouzet, E. *Chem. Mater.* **2000**, 12, 2902. (b) Cao, L.; Kruk, M. *J. Colloid Interface Sci.* **2011**, DOI: 10.1016/j.jcis.2011.05.076.
- (19) **Gas Sorption.** Surface area, mesopore dimensions, and pore volumes were determined by nitrogen physisorption at 77 K (ASAP 2010, Micromeritics Co., Norcross, GA). The specific surface area was deduced using the BET method between 0.05 and 0.2  $P/P_0$ . The total mesopore volume was taken at 0.98  $P/P_0$ . Pore size was determined using an NLDFT kernel developed for silica (Autosorb 1.53 software, Quantachrome Instruments, Boynton Beach, FL) assuming cylindrical pores (equilibrium model). **SAXD.** The powder diffraction measurements were done at the SAXS beam line I711 at MAXLAB, Lund, Sweden.<sup>17</sup> No background subtraction was done. The raw data were normalized to the first order (10) peak. **SEM.** SEM micrographs were recorded with a JEOL JSM-6700 microscope operating at 10 kV. The samples were sputter coated with gold before examination. **TEM.** TEM micrographs were recorded with a JEM3000FX operated at 300 kV.